

Thermal Management of Electronic devices using Phase Change Materials (PCM): Effect of PCM Volume Fraction

Mohammed Waseem Nawaz¹, Dr.P.Srinivasulu² Dr. Singaram Lakshmanan³ Mr. B. Nagaraju⁴ Mr. M. Anil Kumar⁵

1. M. Tech in Thermal Engineering, Department of Mechanical Engineering, Vaagdevi College of Engineering, Bollikunta, Warangal Urban-506005. The college is UGC autonomous, approved by AICTE, and has permanent affiliation to JNTU Hyderabad.
2. Professor and Head, Department of Mechanical Engineering, Vaagdevi College of Engineering, Bollikunta, Warangal Urban-506005. The college is UGC autonomous, approved by AICTE, and has permanent affiliation to JNTU Hyderabad.
3. Associate Professor, Department of Mechanical Engineering, Vaagdevi College of Engineering, Bollikunta, Warangal Urban-506005. The college is UGC autonomous, approved by AICTE, and has permanent affiliation to JNTU Hyderabad.
4. Assistant Professor, Department of Mechanical Engineering, Vaagdevi College of Engineering, Bollikunta, Warangal Urban-506005. The college is UGC autonomous, approved by AICTE, and has permanent affiliation to JNTU Hyderabad.
5. Assistant Professor, Department of Mechanical Engineering, Vaagdevi College of Engineering, Bollikunta, Warangal Urban-506005. The college is UGC autonomous, approved by AICTE, and has permanent affiliation to JNTU Hyderabad.

ABSTRACT

This experimental study investigates passive cooling of electronic devices using fin heat sinks made of phase change material (PCM) to prolong operating time, maintain sufficiently low temperatures, and enhance functionality. Paraffin wax serves as the PCM and is filled into aluminum heat sinks. Aluminum fins are used as a thermal conductivity enhancer (TCE) since PCM has low thermal conductivity. Uniform heat flux is applied to both finned and un-finned heat sinks, with the latter serving as a baseline. Volume fractions of PCM vary from 0.00 to 1.00 in each heat sink to assess thermal performance. The study reports thermal performance at uniform heat fluxes to extend operating time for various set point temperatures (SPTs) and compare latent heat phase duration for different heat sinks. Results indicate that a finned array heat sink filled with a PCM volumetric fraction of 1.00 achieves the best thermal performance in terms of operating time.

1. INTRODUCTION

Effective thermal management of electronic equipment is crucial in the modern era, especially with the increasing demand for compact design and high functionality. The heat generated by compact circuitry requires efficient dissipation techniques, often utilizing active cooling methods. However, active cooling methods such as miniature centrifugal fans have drawbacks including space constraints, noise levels, high maintenance, and increased power requirements. Passive thermal management techniques, particularly those employing heat sinks filled with phase change materials (PCMs), offer promising solutions to extend equipment operating

lifespan and enhance functional performance. Numerous studies have explored passive cooling of portable electronic devices using PCM-filled heat sinks, both experimentally and numerically.

Tan and Tso [6] conducted experiments on cooling mobile devices, such as personal digital assistants and wearable computers, using a heat storage unit filled with PCM. Heat dissipated through the chips was absorbed by the PCM, resulting in effective cooling. Tan and Fok [7] performed numerical simulations on PCM-filled heat storage units for thermal management of mobile phones, demonstrating temperature control at different power levels. Kandasamy et al. [8] contributed both experimentally and numerically to the study of PCM packages for cooling electronics, investigating various parameters such as power levels, orientation, and charging/discharging cycles. Their research highlighted the improved cooling performance of PCM heat sinks compared to those without PCM, particularly in unsteady cases. Krishnan et al. [9] proposed a novel hybrid heat sink concept for transient thermal management of electronics, combining active and passive cooling approaches.

The investigation into passive cooling of electronic devices using fin heat sinks made of phase change material (PCM) to extend operating time, ensure sufficiently low temperature, and enhance functionality of installed features is the focus of the current experimental study. Paraffin wax is employed as a PCM and filled in heat sinks made of aluminum, with aluminum fins utilized as a thermal conductivity enhancer (TCE) due to PCM's low thermal conductivity. A uniform heat flux is applied to both finned and un-finned heat sinks, with the latter serving as a baseline for comparison. Varying volume fractions of PCM are tested for each heat sink to assess thermal performance. The study reports thermal performance at uniform heat fluxes to enhance operating time for various set point temperatures (SPTs) and to compare the latent heat phase duration for different heat sinks tested. The results indicate that a finned array heat sink filled with a PCM volumetric fraction of 1.00 achieves the best thermal performance in terms of operating time.

Several experimental and numerical studies have been conducted to investigate the heat transfer mechanisms and thermal management efficiency of PCM-based heat sinks for cooling electronic components. Yin et al. [10] performed computational analysis to study the effects of natural convection of melt on a parallel-plate fin submerged in PCM. Composite PCMs were investigated by Tan and Tso [6], who demonstrated excellent absorbability and high thermal conductivity of paraffin wax with expanded graphite. Gharbi et al. [11] presented experimental comparisons of different configurations of PCM-based heat sinks, highlighting the effectiveness of graphite matrix-filled PCM in enhancing system performance. Numerical proposals for improving heat transfer in composite heat sinks filled with PCM were made by Akhilesh et al. [12], while Fok et al. [13] conducted experimental studies on PCM-filled heat sinks for portable hand-held electronic devices. Saha et al. [15] numerically examined the optimum distribution of fins in PCM-based heat sinks and found stability in temperature to be proportional to the amount of PCM used. Additionally, Alshaer et al. [17] investigated the thermal management of electronic equipment using a hybrid composite system comprising carbon foam and PCM/nano-composite, reporting enhanced heat transfer efficiency. Alawadhi and Amon [18] reported on the energy management performance of thermal control units for electronic packages, emphasizing the importance of thermal conductivity enhancers. Mahmoud et al. [23] experimentally investigated various heat sink configurations and PCM types, with numerical optimization studies on PCM-based pin-fin heat sinks conducted by Pakrouh et al. [24].

Geometric optimization was conducted using the Taguchi method coupled with numerical simulation. Parameters such as fin thickness, fin height, base thickness, and number of pins of a pin-fin PCM-based heat sink were studied for optimization, with paraffin RT44HC used as the PCM. The authors concluded that the number of pins and pin height make significant contributions to energy management enhancement compared to base thickness. The selection of an optimized PCM-based heat sink with a thermal conductivity enhancer (TCE) is currently a major area of research for improving the thermal management of electronic devices across various heat input levels.

The use of paraffin wax as a phase change material in passive cooling applications for electronics has garnered significant interest among researchers. Therefore, the present experimental study explores the effect of volume fraction of PCM in a finned array heat sink by filling the heat sink with three different volumetric fractions.

Experimental Setup: The experimentation is conducted with a typical heat input, utilizing a dry heat block to simulate the heat generated by an electronic device. The schematic and pictorial diagram of the experimental setup are shown in Fig. 1 and 2, respectively. The setup includes a heat sink with a fin array configuration filled with PCM, thermocouples, a data acquisition system, and a dry heat block. Temperatures at different points on the heat sink are measured using high precision J-type thermocouples (Keysight). In total, nine calibrated thermocouples are inserted at different locations to measure the heater temperature and heat sink temperature, providing a better understanding of temperature distribution.

A $154 \times 194 \text{ mm}^2$ plate heater (Model BSH1004-E SN: AS-BSH4-1537 220V) is utilized to simulate heat generation in an electronic device, adhered to the base of the heat sink with an area of $100 \times 60 \text{ mm}^2$. An AC power supply of 220V is employed to provide the required power to the heater, with an input heat flux of 3.68 kW/m^2 applied at the base of the heat sink. All thermocouples are highly calibrated according to ASTM standards [25] within a temperature range of -40°C to 150°C , with a maximum variation of $\pm 0.1^\circ\text{C}$. A Data Acquisition System (Keysight 34972A SN: MY49020379) is used to record the temperature at 5-second intervals during the experiment.

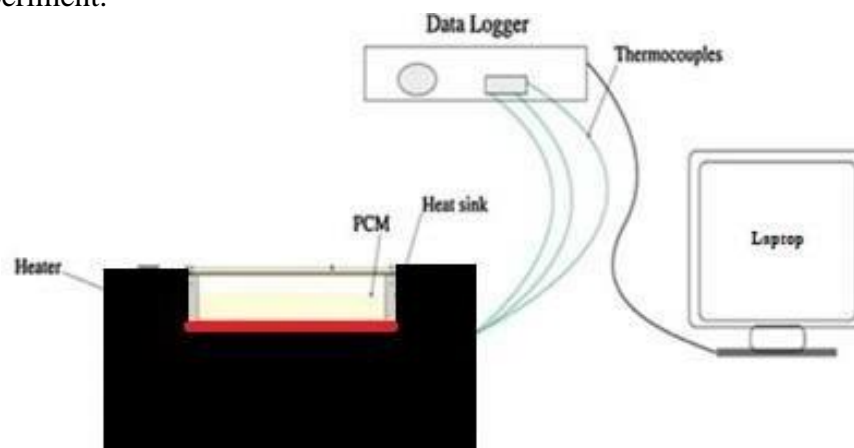


Figure 1. Schematic representation of experimental setup.

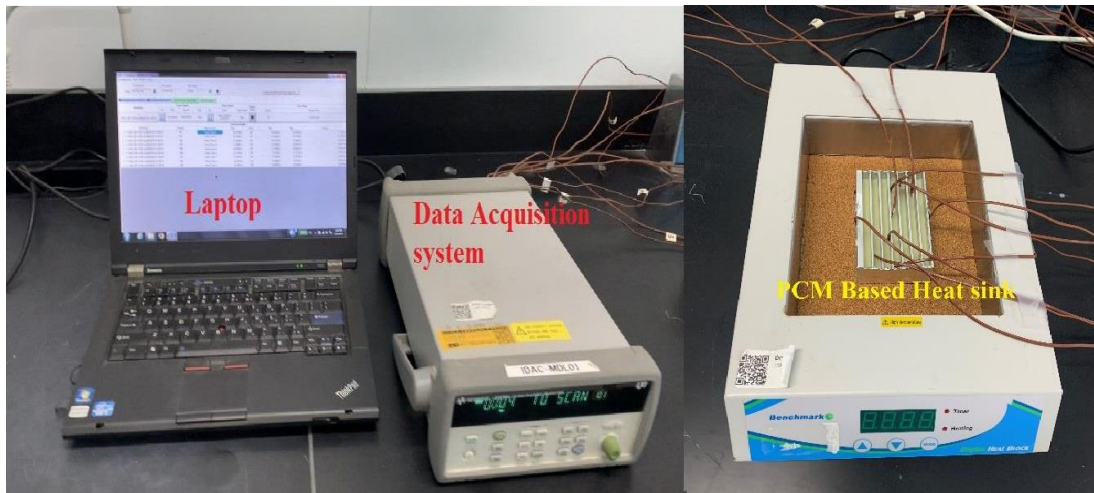


Figure 2. Experimental setup.

Nomenclature:

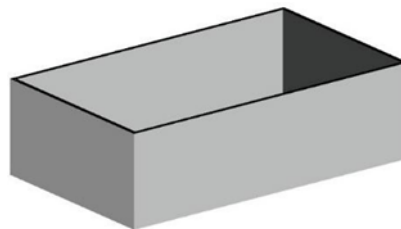
- PCM: Phase Change Material
- TCE: Thermal Conductivity Enhancer
- SPT: Set Point Temperature
- TM: Thermal Management
- CNC: Computer Numerical Control
- T: Thermocouple (inside PCM)
- W: Thermocouple (at the heat sink side walls)
- H: Thermocouple (at heat sink base)
- VS: Total volume of heat sink
- Vf: Total volume of fins

Greek Symbols:

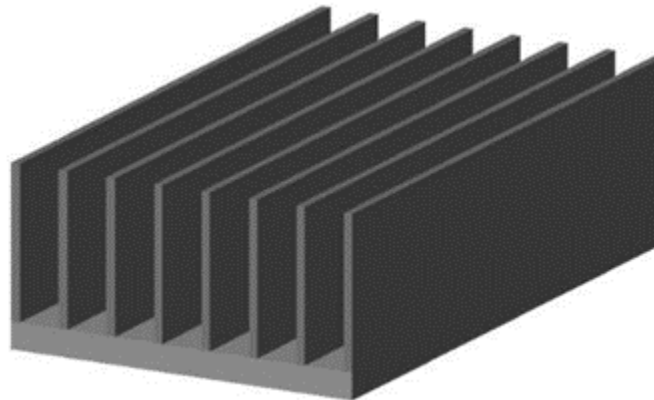
- Ψ : Volumetric Fraction of PCM
- Γ : Specific Volume of PCM

Heat Sink Configurations:

Two different configurations of heat sinks filled with PCM (paraffin wax) are used. A heat sink with no fins at $\Psi = 0.00$ and $\Psi = 1.00$ is tested to establish a baseline comparison. Additionally, a heat sink with a finned array, with a fin thickness of 1.5 mm, is depicted in Fig. 3.



(a) No fin Heat sink



(a) Fin array Heat sink

Figure 3: Isometric views of heat sinks tested in this experiment

H: Thermocouple (at heat sink base) VS: Total volume of heat sink Vf: Total volume of fins
Greek Symbols: Ψ : Volumetric fraction of PCM Γ : Specific volume of PCM

Heat Sink Configurations:

Two different configurations of heat sinks filled with PCM (paraffin wax) are used. A heat sink with no fins at $\Psi = 0.00$ and $\Psi = 1.00$ is tested to establish a baseline comparison. Additionally, a heat sink with a finned array, with a fin thickness of 1.5 mm, is depicted in Fig. 3.

Previously, Saha et al. [15] reported that the 8% volume fraction of TCE had optimum fin distribution of 2 mm thick fin, however, Baby and Balaji [20] found that the 9% volume fraction (volume of fin to total volume of the heat sink) of TCE gives the best thermal performance. Aluminum is selected as the TCE due the good thermal conductivity and light weight. Paraffin wax [26] is used as a PCM and four different volume fractions ($\Psi = 0.00$, $\Psi = 0.33$, $\Psi = 0.66$, and $\Psi = 1.00$) are used for the heat sink by using Eq. (1).

$$T = \Gamma_{\text{PCM}} / (VS - Vf) \text{-(1)}$$

The heater surface is insulated with rubber material to prevent heat loss to the environment, and an area of $100 \times 60 \text{ mm}^2$ is cut out for placing the heat sink at the center, which is dimensioned with an area of $100 \times 60 \text{ mm}^2$ and a height of 30 mm. To observe the physical state of PCM, the top surface of the heat sink is left uncovered. Table 1 provides the material properties employed in the present investigation. The dimensions of materials used for the heat sink are mentioned in Table 2.

The finned array with a 1.5mm fin thickness and a height of 25.5mm is manufactured by a CNC milling machine from an aluminum block of dimensions $114 \times 65 \times 35 \text{ mm}^3$, with a total of 8 parallel fins as an array. The general dimensions of the plate finned array heat sink are shown in Fig. 4.

Table 1: Properties of Materials Employed in the Presented Experiment

Material	Thermal Conductivity (W/m K)	Specific Heat (kJ/kg K)	Latent Heat (kJ/kg)	Melting Point (°C)	Density (kg/m ³)
Paraffin Wax	0.167 (Liquid)	2.8	173.6	56-58	790 (Liquid)
	0.212 (Solid)			880 (Solid)	
Aluminum	202.37	0.871	-	660.37	2719

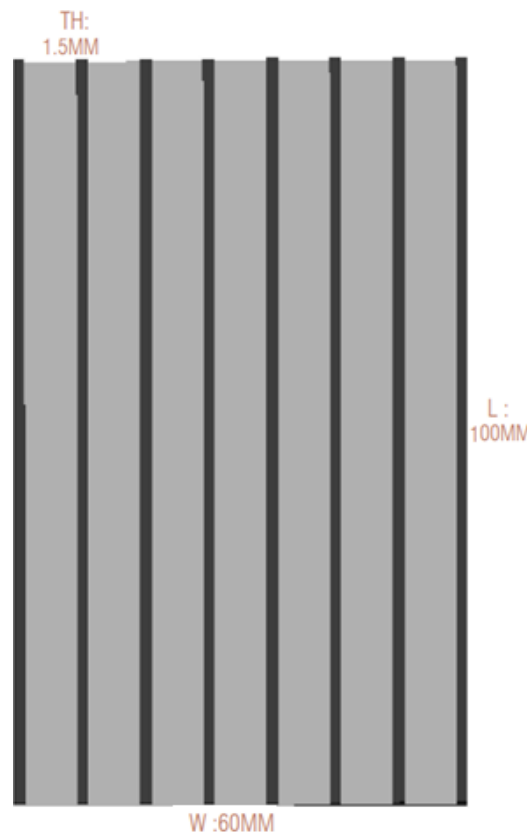
Table 2: Material Specifications Used for Making the Heat Sink Assembly

Sr. No.	Materials Used	Dimensions (mm)
1	Heat Sink	100 x 60 x 30

Thermocouple Positions

To observe the melting and solidification of paraffin wax, thermocouples T1 to T5 are inserted at various positions along the spatial direction. T1 and T2 are fixed at a height of 5 mm from the bottom, T3 and T4 are placed at 10 mm, and T5 is positioned at 15 mm.

Thermocouples are also affixed to the side walls of the heat sink to measure temperature distribution along the boundary. Thermocouples W1 to W2 are inserted into the side wall surface of the heat sink at a height of 20 mm. Two thermocouples, H1 and H2, are placed at the base of the heat sink between the plate heater and the base of the heat sink, equidistant from each other. Additionally, a thermocouple is positioned outside to record the ambient room temperature. Detailed positions of the thermocouples are illustrated in Fig. 5.



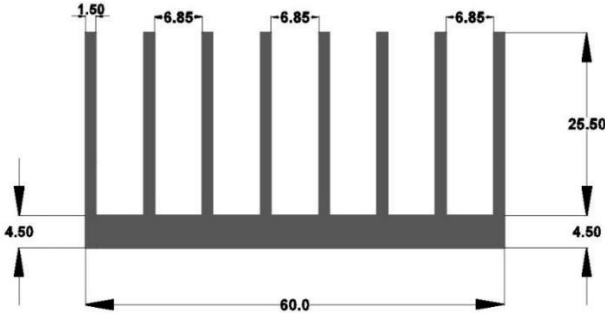


Figure 4: Dimensions of 1.5 mm thick fin heat sink.

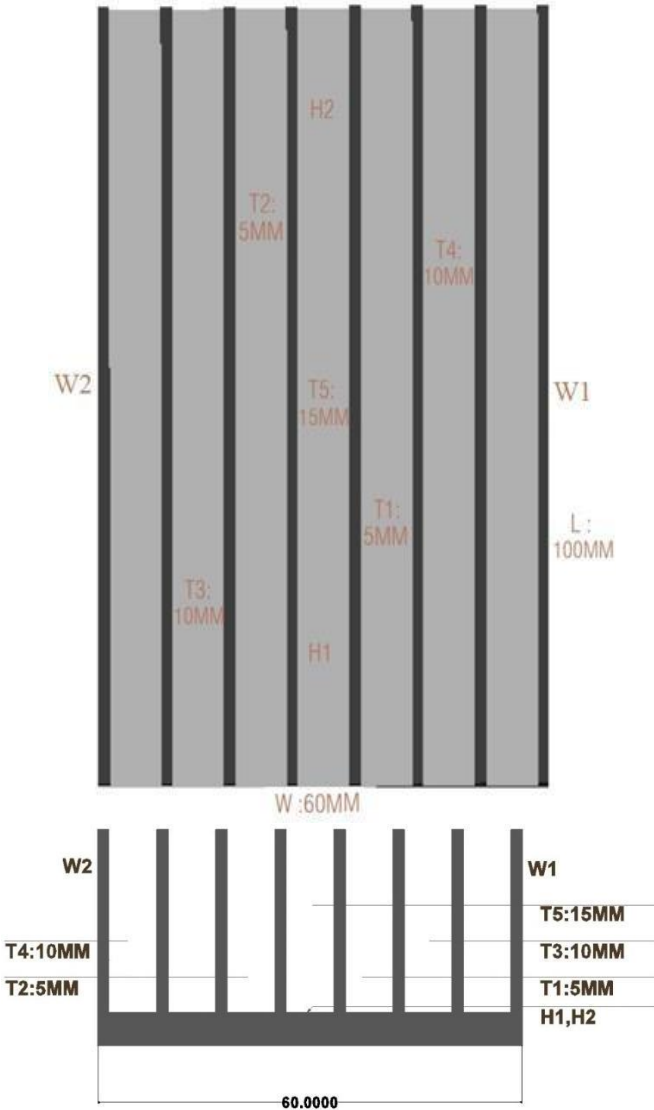


Figure 5: Diagram represents the positions of thermocouples in a heat sink.

3. Results and Discussion

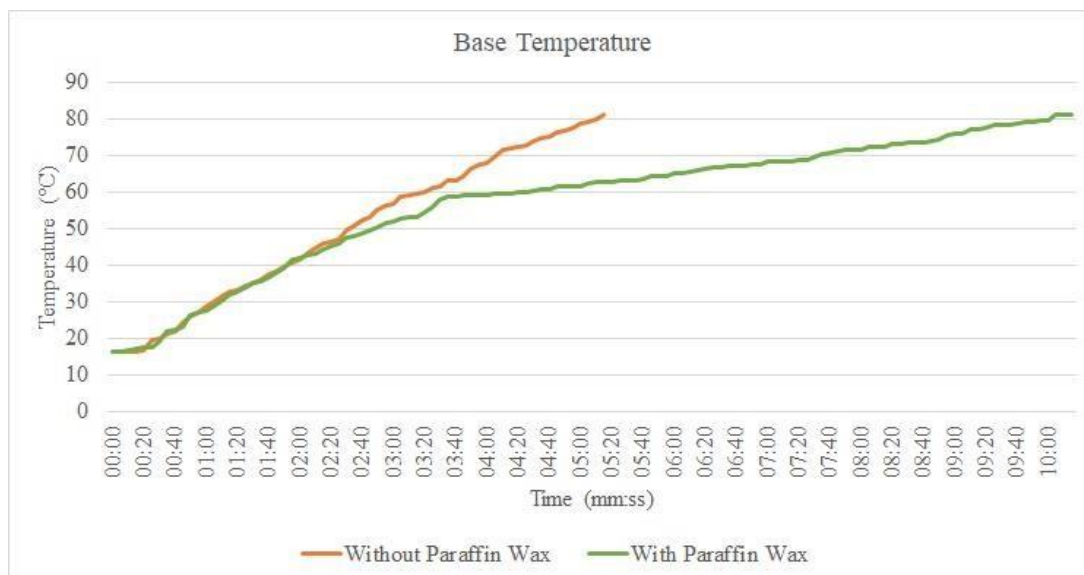
Baseline Comparison

A comparison of the base temperature and side wall temperature with and without PCM at an input heat flux of 3.68 kW/m^2 is presented in Fig. 6(a) and (b) respectively. The green and yellow-colored lines represent the transient temperature variation of a heat sink with no fins filled with PCM (paraffin wax), while the orange-colored line represents the temperature variation of a heat sink without PCM.

The average values of thermocouples H1 and H2 are taken to record the heat sink base temperature, and the average values of thermocouples W1 and W2 are used to represent the side wall temperature. To reach a base temperature of $52 \text{ }^\circ\text{C}$ and $60 \text{ }^\circ\text{C}$, the heat sink without PCM takes 02:40 min and 03:20 min respectively, whereas it takes 03:00 min and 04:35 min for a heat sink filled with PCM (Fig. 13a). Similar trends in temperature variation are observed at the side wall of the heat sink filled with PCM and without PCM. Fig. 6(b) shows that to reach a temperature of $50 \text{ }^\circ\text{C}$ and $60 \text{ }^\circ\text{C}$, it takes 03:00 min and 03:55 min respectively for a heat sink without PCM. Whereas, for a heat sink filled with PCM, it takes 03:15 min and 05:30 min respectively at the side wall (recorded at the height of 10 mm).

This reflects that the surface and the wall temperatures increase rapidly when the heat sink is not filled with PCM, which is extremely undesirable for an electronic device used for a prolonged duration. The sharp increase in temperature of the heat sink without PCM also adversely affects the life and reliability of portable electronic devices. In this experiment, heat flux is provided for 60 min, and the temperature rises to $60 \text{ }^\circ\text{C}$ at the base of the heat sink filled with PCM.

As the melting temperature of paraffin wax used in this experiment is $56\text{--}58 \text{ }^\circ\text{C}$, the green and yellow-colored curve represents the sensible heating before phase change, and the temperature remains under desirable conditions for better thermal management of electronics.



(a) base temperature



(b) wall temperature.

Figure 6: Comparison of temperature-time with and without PCM at 3.68 kW/m²



Figure 8: Temperature-time distribution with different Ψ of PCM at 3.68 kW/m² for finned array heat sink

The spatial distribution of temperature inside the finned array heat sink is depicted in Fig. 9. The plate heater positioned at the base of the heat sink serves as the reference point for temperature measurement. Additionally, in the vertical direction of the heat sink, five thermocouples, namely T1 & T2, T3 & T4, and T5, are inserted at heights of 5 mm, 10 mm, and 15 mm, respectively. The average values of these thermocouples are utilized to graphically represent the melt front of the molten PCM inside the heat sink. The temperature depicted in

these figures is recorded after time intervals of 20 min, 40 min, and 60 min for enhanced comprehension.

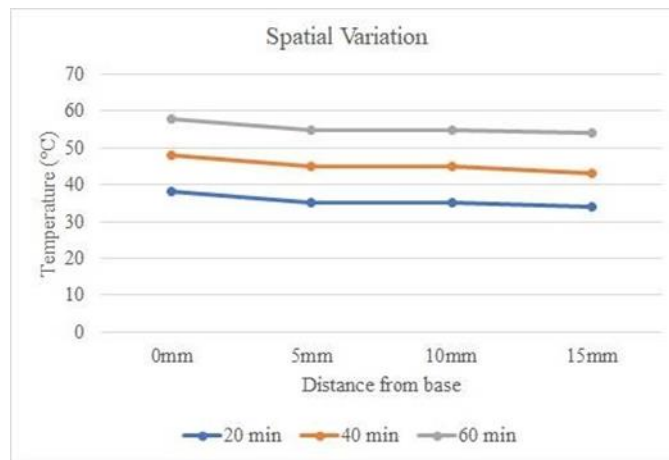


Figure 9: Spatial distribution of temperature inside the PCM, for Finned array heat sink.

The spatial distribution of temperature after reaching the base indicates that there is not a significant variation in temperature inside the PCM.

Temperature Distribution within the Molten PCM (Paraffin Wax)

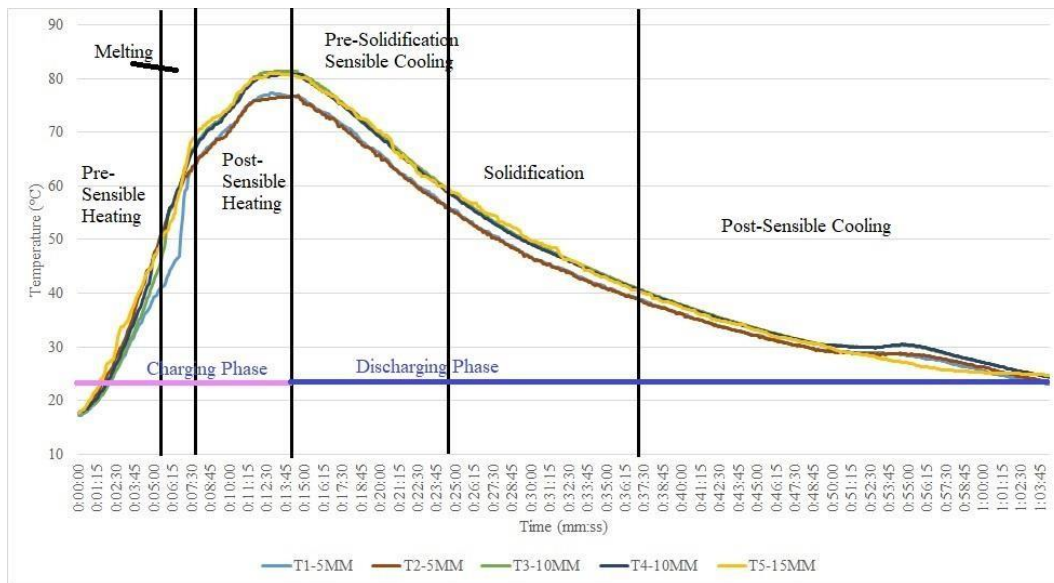


Figure 10: Temperature distribution at different locations

The temperature-time history within the molten PCM for the finned array heat sink is depicted in Fig. 10 at a heat flux of 3.68 kW/m². The average values of T1 & T2, T3 & T4, and T5 located at heights of 5 mm, 10 mm, and 15 mm respectively are recorded. The first 13:20 min

represents the charging phase (melting phase), while the remaining 50 min represent the discharging or solidification phase.

From Fig. 10, it is observed that at 13:30 min, the recorded temperatures by T1 to T5 are 76.9 °C, 76.4 °C, 81.2 °C, 80.6 °C, and 80.7 °C. The figure is divided into five regions corresponding to various stages of the heating and cooling phases of the PCM.

Enhancement in the Operation Time of PCM Based Finned Array Heat Sinks

Operational times for various PCM-based heat sinks are presented in Table 3.

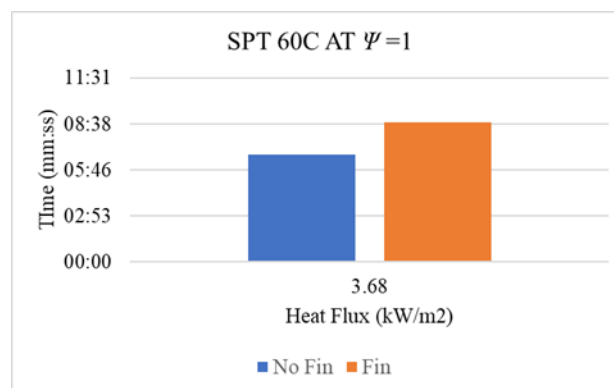
Table 3:

Heat Flux (kW/m ²)	Volume Fraction	Type of Heat Sink	Time for SPT (60 °C)	Time for SPT (65 °C)	Time for SPT (70 °C)
3.68	$\Psi = 0$	No Fin	03:20	03:45	04:05
		Fin	04:25	06:00	07:35
3.68	$\Psi = 0.33$	No Fin	08:35	09:05	10:15
		Fin	08:25	09:00	09:40
3.68	$\Psi = 0.66$	No Fin	06:40	07:25	08:40
		Fin	07:05	07:45	08:50
3.68	$\Psi = 1.00$	No Fin	06:45	07:30	08:20
		Fin	08:45	09:25	10:40

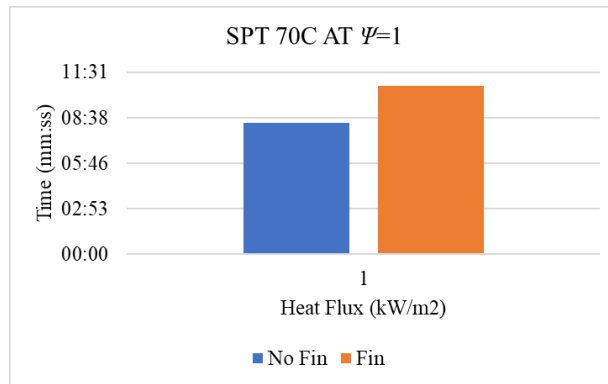
Observing the data, a trend emerges where the time required to reach specific heat flux values varies as the volumetric fraction shifts from $\Psi = 0.00$ to $\Psi = 1.00$ for each heat sink. Upon closer examination, it becomes apparent that the finned heat sink requires more time at $\Psi = 0.33$ than at $\Psi = 0.66$ of PCM. However, at $\Psi = 1.00$, it demonstrates superior thermal performance compared to $\Psi = 0.33$ and $\Psi = 0.66$ fin heat sinks.

Figures 11a and 11b depict the time taken for both no fin and finned array heat sinks to reach the SPTs of 60°C and 70°C, respectively.

It is notable that the finned array heat sinks take longer to reach the SPTs of 60°C and 70°C compared to the no fin heat sinks. This increased time in the case of finned arrays can be attributed to the optimized pitch and number of fins corresponding to the volume fraction of TCE.



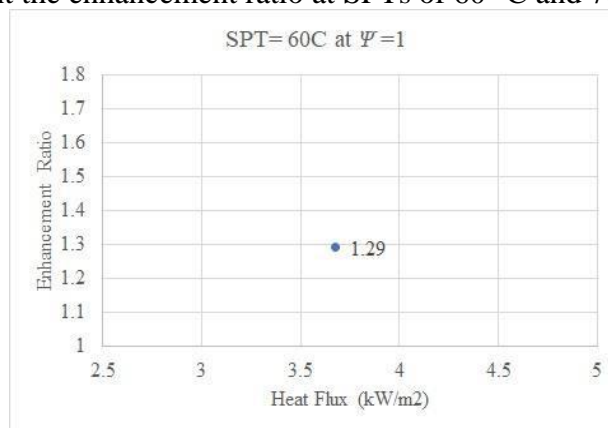
(a)



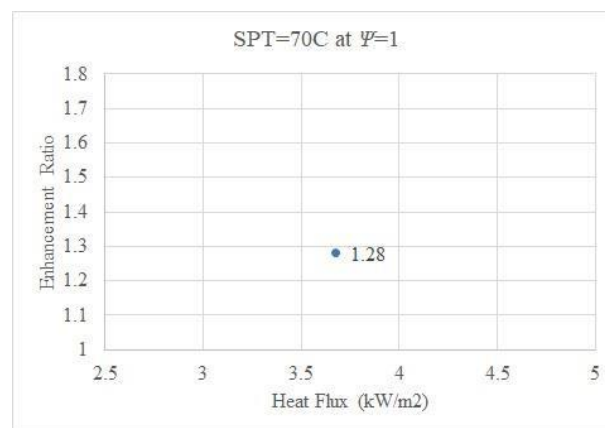
(b)

Figure 11: Time to reach a SPT (a) 60 °C (b) 70 °C

Fig. 12 a and b represent the enhancement ratio at SPTs of 60 °C and 70 °C, respectively.



(a)

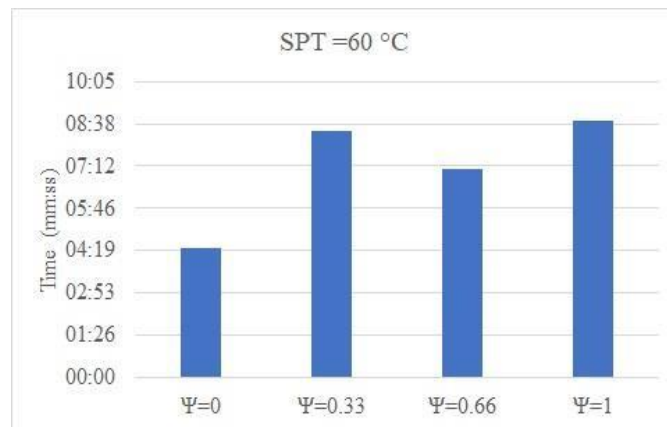


(b)

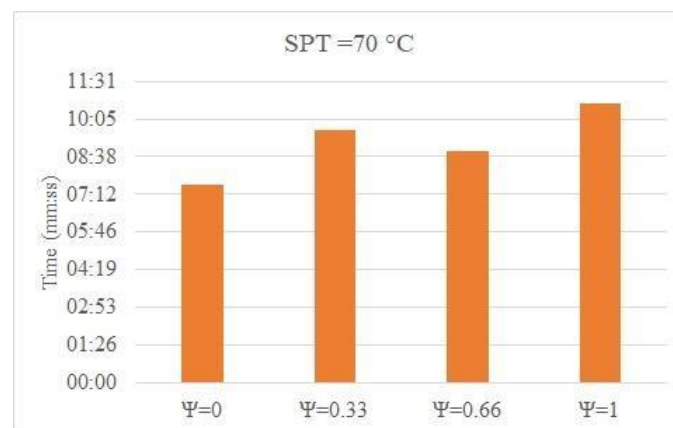
Figure 12: Enhancement in operating time due to presence of fins for a base temperature of (a) 60 °C and (b) 70 °C.

The enhancement in operational duration of a heat sink can be quantified using the enhancement ratio, which is calculated as the ratio of the time taken by the heat sink with fins to that of a heat sink without fins to reach a critical SPT. For instance, an enhancement ratio of 1.29 indicates improved thermal management of portable electronic packages at 60°C and 3.68 kW/m² with $\Psi = 1.00$ in the heat sink. This signifies a significant enhancement in the thermal performance of PCM-based heat sinks with a constant volume fraction of TCE.

Furthermore, based on the data presented in Table 3, it can be observed that at $\Psi = 1.00$, the finned heat sink demonstrates the best thermal performance in terms of operating time compared to other heat sinks tested in this experiment. The time required to reach critical SPTs of 60°C and 70°C is illustrated in Figures 13a and 13b, respectively, for different volumetric fractions of PCM.



(a)

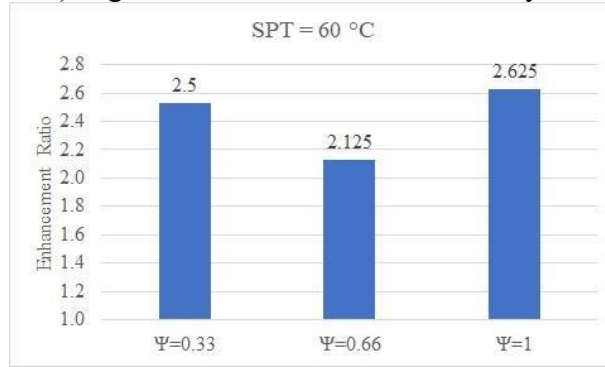


(b)

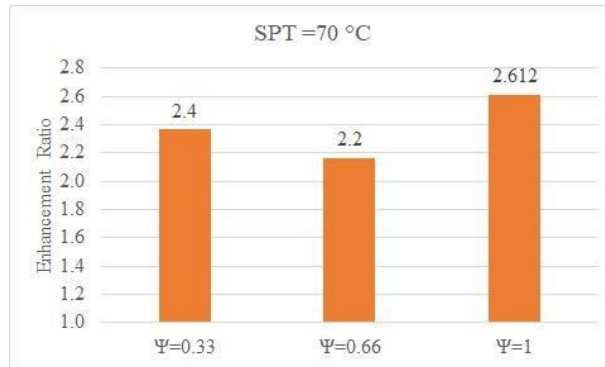
Figure 13: Time to reach a SPTs at various heat inputs for the finned heat sink at (a) 60 °C and (b)70 °C.

The bars presented in the figures depict the time required to reach a specific set point temperature (SPT) for the finned heat sink, highlighting that at a higher volumetric fraction $\Psi = 1.00$ (fully filled with PCM), the time is the longest compared to lower volume fractions. Figures 14a and 14b provide a clear depiction of the effect of volume fractions ($\Psi = 0.33$, $\Psi = 0.66$, and $\Psi = 1.00$) of PCM in terms of the enhancement ratio.

From Figures 14a and 14b, it is evident that the enhancement in operation time to reach a base temperature (60°C and 70°C) is greater when the heat sink is fully filled ($\Psi = 1.00$).



(a)



(b)

Figure 14: Enhancement in operating time at different volume fractions at (a) 60°C & (b) 70°C .

The enhancement ratio of finned heat sinks at $\Psi = 0.00$ and $\Psi = 1.00$ of PCM is illustrated in Figure 15. The figure provides a visual representation of the thermal performance of PCM in storing heat generated by electronic equipment when filled within the heat sink, compared to an unfilled heat sink. The enhancement ratio, defined as the ratio of the time taken to reach a specific set point temperature (SPT) of a finned heat sink filled with PCM ($\Psi = 1.00$) to that of an unfilled heat sink ($\Psi = 0.00$), is depicted.

Clear evidence from Table 3 demonstrates that the thermal efficiency of a fully filled PCM-based heat sink surpasses that of other configurations. As a consequence, considering the critical base temperatures of various electronic devices that can withstand without failure of their design features, it is observed from the figure that the maximum enhancement ratio is achieved at lower SPTs, attributable to the maximum time taken to complete the latent heat phase. Enhancement ratios of 2.625 and 2.6 are obtained at an input heat flux of 3.68 kW/m^2

for SPTs of 60°C and 70°C, respectively. A decreasing trend at higher SPTs is attributed to the rapid increase in temperature during the post-melting phase.

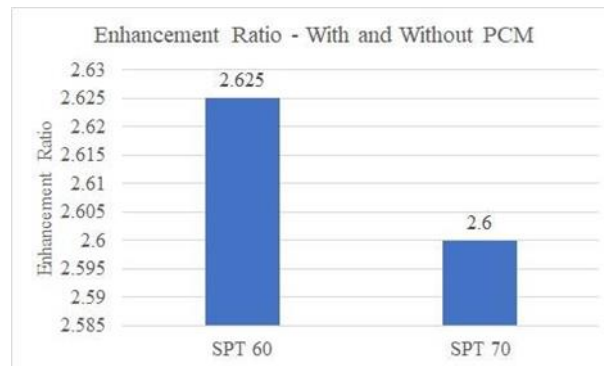


Figure 15 illustrates the enhancement ratio of finned heat sinks for different Set Point Temperatures (SPTs) of PCM at $\Psi = 0.00$ and $\Psi = 1.00$.

Conclusion

In conclusion, phase change materials (PCMs) play a crucial role in managing the thermal characteristics of electronic equipment by regulating hot spots and ensuring a more uniform temperature distribution within components. Future research should focus on the stability and suitability of PCMs during extended usage periods, as well as the development of practical design procedures to assist designers in implementing PCM cooling systems.

The experiments conducted in this study evaluated the effect of finned array PCM-based heat sinks for an input heat flux of 3.68 kW/m². With low thermal conductivity PCM, this experimental study demonstrates the impact of finned array heat sinks for various volumetric fractions of paraffin wax ($\Psi = 0.00$, $\Psi = 0.33$, $\Psi = 0.66$, and $\Psi = 1.00$). Key findings of this experiment are summarized below:

1. Inclusion of paraffin wax reduces the base temperature of the heat sink, thereby improving the operation time of electronic devices.
2. An enhancement ratio of 1.296 is achieved for an SPT of 60 °C at 3.68 kW/m² for the heat sink compared to a heat sink without fins.
3. It takes 08:45 min and 10:40 min to reach set point temperatures of 60 °C and 70 °C, respectively, for the finned heat sink at a volumetric fraction of $\Psi = 1.00$.
4. The effectiveness of a PCM-based heat sink depends on the amount of PCM and the number of fins.
5. Finned array heat sinks demonstrate better heat transfer performance compared to no-fin heat sinks at $\Psi = 0.33$ and $\Psi = 1.00$.
6. An enhancement ratio of 2.65 is achieved against a heat flux of 3.68 kW/m² for a finned array heat sink at an SPT of 60 °C compared to with and without PCM.

References:

1. Grimes, R., Walsh, E., Walsh, P. (2010). Active cooling of a mobile phone handset. *Appl. Therm. Eng.*, 30(16), 2363–2369.
2. Peles, Y., et al. (2005). Forced convective heat transfer across a pin fin micro heat sink. *Int. J. Heat Mass Transf.*, 48(17), 3615–3627.

3. Ng, K.C., Yap, C.R., Chan, M.A. (2008). A universal performance chart for CPU cooling devices. *Heat Transfer Eng.*, 29(7), 651–656.
4. Walsh, E., et al. (2008). Thermal management of low-profile electronic equipment using radial fans and heat sinks. *J. Heat Transfer*, 130(12), 125001.
5. Kandasamy, R., Wang, X.-Q., Mujumdar, A.S. (2008). Transient cooling of electronics using phase change material (PCM)-based heat sinks. *Appl. Therm. Eng.*, 28(8–9), 1047–1057.
6. Tan, F.L., Tso, C.P. (2004). Cooling of mobile electronic devices using phase change materials. *Appl. Therm. Eng.*, 24(2–3), 159–169.
7. Tan, F.L., Fok, S.C. (2007). Thermal management of mobile phone using phase change material. *IEEE 9th Electronics Packaging Technology Conference 2007*, 836–842.
8. Kandasamy, R., Wang, X.-Q., Mujumdar, A.S. (2007). Application of phase change materials in thermal management of electronics. *Appl. Therm. Eng.*, 27(17–18), 2822–2832.
9. Krishnan, S., Garimella, S.V., Kang. (2004). A Novel hybrid heat sink using phase change materials for transient thermal management of electronics. *IEEE Inter Society Conference on Thermal Phenomena*, 310–318.
10. Yin, H., et al. (2008). Experimental research on heat transfer mechanism of heat sink with composite phase change materials. *Energy Convers. Manage.*, 49(6), 1740–1746.
11. Gharbi, S., Harmand, S., Jabrallah, S.B. (2015). Experimental comparison between different configurations of PCM based heat sinks for cooling electronic components. *Appl. Therm. Eng.*, 87, 454–462.
12. Akhilesh, R., Narasimhan, A., Balaji, C. (2005). Method to improve geometry for heat transfer enhancement in PCM composite heat sinks. *Int. J. Heat Mass Transf.*, 48(13), 2759–2770.
13. Fok, S.C., Shen, W., Tan, F.L. (2010). Cooling of portable hand-held electronic devices using phase change materials in finned heat sinks. *Int. J. Therm. Sci.*, 49(1), 109–117.
14. Setoh, G., Tan, F.L., Fok, S.C. (2010). Experimental studies on the use of a phase change material for cooling mobile phones. *Int. Commun. Heat Mass Transfer*, 37(9), 1403–1410.
15. Saha, S.K., Srinivasan, K., Dutta, P. (2008). Studies on optimum distribution of fins in heat sinks filled with phase change materials. *J. Heat Transfer*, 130(3), 034505.
16. Suresh, S., et al. (2013). Experimental investigation of PCM-based heat sink with different configurations of internal fins. *International Conference on Advance Research in Mechanical, Aeronautical and Civil 2013*, 54–59.
17. Alshaer, W.G., et al. (2015). Thermal management of electronic devices using carbon foam and PCM/nano-composite. *Int. J. Therm. Sci.*, 89, 79–86.
18. Alawadhi, E.M., Amon, C.H. (2000). Performance analysis of an enhanced PCM thermal control unit. *IEEE Inter Society Conference on Thermal Phenomena*, 283–289.
19. Alawadhi, E.M., Amon, C.H. (2003). PCM thermal control unit for portable electronic devices: experimental and numerical studies. *IEEE Transactions on Components and Packaging Technologies*, 116–125.
20. Baby, R., Balaji, C. (2012). Experimental investigations on phase change material based finned heat sinks for electronic equipment cooling. *Int. J. Heat Mass Transf.*, 55(5–6), 1642–1649.

21. Baby, R., Balaji, C. (2012). Thermal management of electronics using phase change material based pin fin heat sinks. 6th European Thermal Sciences Conference, Journal of Physics 2012, IOP Publishing.
22. Baby, R., Balaji, C. (2013). Thermal optimization of PCM based pin fin heat sinks: an experimental study. *Appl. Therm. Eng.*, 54(1), 65–77.
23. Mahmoud, S., et al. (2013). Experimental investigation of inserts configurations and PCM type on the thermal performance of PCM based heat sinks. *Appl. Energy*, 112, 1349–1356.
24. Pakrouh, R., et al. (2015). A numerical method for PCM-based pin fin heat sinks optimization. *Energy Convers. Manage.*, 103, 542–552.
25. Burns, G.W., et al. (1993). Temperature-electromotive force reference functions and tables for the letter-designated thermocouple types based on the ITS-90. NASA STI/Recon Technical Report N, 93.
26. EMD Millipore. (2016). Histosec-pastilles. Available from: http://www.emdmillipore.com/US/en/product/Histosec-pastilles,MDA_CHEM-111609.
27. Put, S., et al. (2001). Die sink electrodischarge machining of zirconia-based composites. *Br. Ceram. Trans.*, 100(5), 207–213.